Epoxy Hybrid Composites Cured with Octaaminophenyl Polyhedral Oligomeric Silsesquioxane

Guang-Xin Chen,[1,2] Lingxia Si,[1] Peng Lu,[2] Qifang Li[1,2]

[1]*State Key Laboratory of Chemical Resource Engineering, Beijing University of Chemical Technology, Beijing 100029, China*
[2]*College of Material Science and Engineering, Beijing University of Chemical Technology, Beijing 100029, China*

Received 2 September 2010; accepted 4 November 2010
DOI 10.1002/app.36400

ABSTRACT: Polyhedral oligomeric silsesquioxane-containing hybrids of epoxy resins are prepared via the cocuring reaction between octaaminophenyl polyhedral oligomeric silsesquioxane (OAPS) and brominated epoxy resin (EP). The gel time, dispersion, thermal properties, mechanical properties, water absorption, and dielectric properties of the OAPS/EP composites are studied. The gel time of the 1 wt % OAPS composites is significantly higher compared with that of the epoxy resin control. Wide angle X-ray diffraction and scanning electron microscopy show that, at the molecular level, the appropriate amount of POSS cages was dispersed in the epoxy matrix because the POSS monomer participated in the crosslinking reaction. The thermal and mechanical properties of the composites are enhanced as 1 wt % OAPS was added to the epoxy system. The water absorption of the 1 wt % OAPS composite significantly declines. The dielectric constant of the 1 wt % OAPS composite is 0.5 less than that of the epoxy resin control in the range of 100 Hz–40 MHz. © 2012 Wiley Periodicals, Inc. J Appl Polym Sci 000: 000–000, 2012

Key words: composites; dielectric properties; resins; mechanical properties

INTRODUCTION

Incorporating inorganic or organometallic segments to polymers to provide improved properties continues to drive the development of new materials.[1–7] Polyhedral oligomeric silsesquioxane (POSS) reagents, monomers, and polymers are emerging as new chemical technologies for the production of nanoreinforced organic–inorganic hybrids,[8–17] and polymers incorporating POSS monomers are becoming the focus of many studies due to their simplicity of processing and the excellent comprehensive properties of this class of hybrid materials.[10–18] The recent development of several families of functional hybrid reagents based on POSS presents tremendous potential for the modification of organic–inorganic hybrid polymers.[8,9] Typical POSS monomers possess cube-octameric frameworks with eight organic corner groups, one or more of which are reactive or polymerizable.

The diversity of the organic groups on the silsesquioxane cage can provide tremendous flexibility for controlling the microstructure of POSS-containing hybrids. Generally, POSS cages can be introduced into polymer systems via copolymerization and physical blending. Copolymerization is an efficient approach to POSS-containing nanocomposites due to the formation of chemical bonds between POSS cages and polymer matrices. Relatively, the nanocomposites prepared via physical blending are less reported due possibly to the unfavorable miscibility (or solubility) of silsesquioxanes in polymers.[19]

Epoxy resins are a class of the most important thermosetting materials and are widely used as adhesives, electronic encapsulating compounds, and matrices of polymer composites, as well as other structural materials, due to their elasticity and strength, excellent chemical resistance, and simplicity in processing. These extensive applications motivate the preparation of organic/inorganic composites of epoxy resins with improved properties. There have been several studies on inorganic–organic hybrids involving epoxy resin and polyhedral oligomeric silsesquioxanes during the past years.[20–26] Lee and Lichtenhan[20] investigated the thermal and viscoelastic properties of cyclohexyl (or cyclopentyl) polyhedral oligomeric silsesquioxane (POSS)-reinforced epoxy resins of bisphenol A. These experiments,

---

Correspondence to: Q. Li (qflee@mail.buct.edu.cn).

Contract grant sponsor: National Natural Science Foundation of China; contract grant number: 20974013.

Contract grant sponsor: Polymer Chemistry and Physics, Beijing Municipal Education Commission (BMEC); contract grant number: XK100100640.

Contract grant sponsor: The National High Technology Research and Development Program of China; contract grant number: 2006AA03Z563.

Journal of Applied Polymer Science, Vol. 000, 000–000 (2012)

which were performed under identical thermodynamic states, revealed that the molecular level reinforcement provided by the POSS cages can significantly retard the physical aging process in the glassy state. Li et al.[22] dispersed multifunctional POSS into an epoxy matrix at the molecular level, even at a POSS weight percent of 25. The epoxy/POSS 75/25 composite exhibited a lower glass transition temperature (T_g) than the neat epoxy resin; the lower T_g was ascribed to the possible incomplete curing of the epoxy due to the inclusion of the POSS cages. In the preparation of glycidylisobutyl POSS-containing epoxy composites, Williams and coworkers[23] observed that a primary liquid–liquid phase separation occurred from the addition of the diepoxide to the POSS-diamine precursor due to the incompatibility between the epoxy precursor and the POSS compound. Laine and coworkers[24,25] investigated the modification of epoxy resin by a series of octafunctional and polyfunctional silsesquioxanes with various R groups (aminophenyl and dimethylsiloxypropylglycidyl ether groups, respectively). The dynamic mechanical properties, fracture toughness, and thermal stability of the epoxy hybrids were considered in terms of the types of R groups, tether structures between the epoxy matrices and POSS cages, and the defects in silsesquioxane cages, among others.

The favorable combination of properties between POSS and polymers requires the optimum dispersion of POSS cubes in the polymeric matrix, which can be adjusted by controlling the type and reactivity of R groups in the POSS cubes. In this study, we prepare nanocomposites using brominated epoxy resins and octaaminophenyl polyhedral oligomeric silsesquioxane (OAPS). The thermal properties, mechanical properties, water absorption, and dielectric properties of the epoxy nanocomposites are also studied.

EXPERIMENTAL

Materials

The brominated epoxy resins (epoxide equivalent: 420–450) were purchased from Guangzhou Hongchang Electronic Material Industry Co. (Guangdong, China). Dicyandiamide (electronic grade) and 2-methyl-imidazole (electronic grade) were purchased from Guangzhou Kawai Electronic Material Co. (Guangdong, China). Tetrahydrofuran (THF) and *N*,*N*-dimethyl formamide (DMF) were purchased from Beijing Chemical Plant, China. Octaaminophenyl polyhedral oligomeric silsesquioxane was prepared according to methods used in previous studies.[27,28] The POSS compounds have a cage-like structure, as shown in Scheme 1.

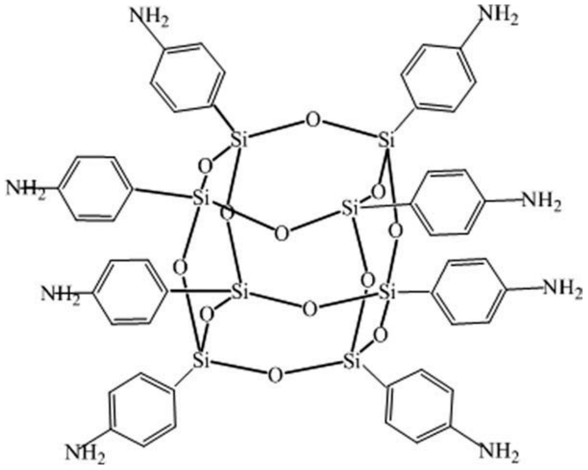

Scheme 1 Structure of OAPS molecule.

Characterization

The gel time of the resin was measured by the fiber-drawing method. While being timed, the mixed solution (about 1 mL) was introduced onto a 170°C hot plate and constantly stirred until it could no longer be drawn into fibers. The interval between the introduction of the resin until it lost its ductility was determined as the gel time of the glue.

Wide-angle X-ray diffraction (XRD) patterns were recorded on a Japan Science D/max-RB automatic diffractometer. All measurements were performed at standard atmospheric pressure and room temperature with nickel-filtered Cu target Kα radiation at 40 kV and 20 mA using a scintillation counter system. Data were recorded in the 2θ range from 5° to 50° at a scanning rate of 5°/min.

An S-4700 scanning electron microscope (SEM) was used to investigate the morphology of the POSS-containing epoxy hybrids. The samples were fractured under cryogenic conditions using liquid nitrogen. The fractured surfaces were immersed in 10 wt % hydrofluoric acid at room temperature for 150 min. If the POSS-rich phase separated out during polymerization, it could be preferentially etched by the solvent, whereas the epoxy matrix phase remained unaffected. The etched specimens were dried to remove the solvents. The fracture surfaces were coated with a 100 Å-thin layer of gold. All specimens were examined at an activation voltage of 20 kV.

Calorimetric measurements were performed on a NETZSCH DSC 200PC in a dry nitrogen atmosphere. All the samples (about 6 mg in weight) were heated from 20 to 200°C and differential scanning calorimetry (DSC) curves were recorded at a heating rate of 20°C/min. The T_g was taken as the midpoint of the capacity change.

Impact strength tests were performed using a CEAST Model RESIL impact tester. The unnotched

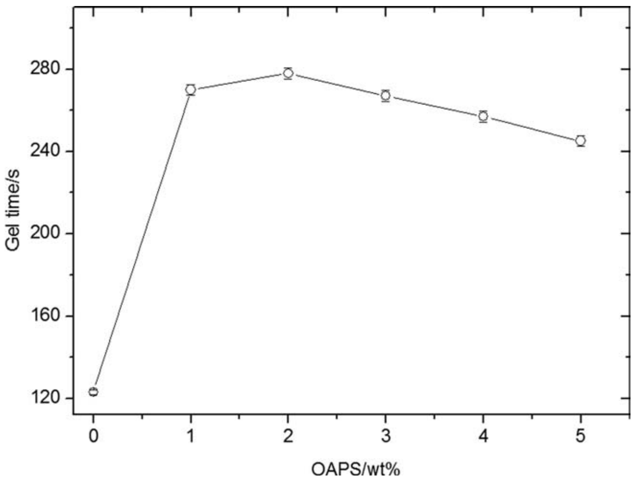

Figure 1 The gel time curve of OAPS/epoxy nanocomposites.

specimen size used was 4 mm × 10 mm × 80 mm. The tensile strength was measured on an Instron Model 1185 test machine according to the recommendations of ASTM D638M2. The specimen size used was 3 mm × 5 mm × 80 mm. All of the mechanical properties were obtained by averaging at least five measurements.

The water absorption of the hybrid composites was tested as follows: The samples were dried at 100°C in a vacuum oven for 1 h. The masses of the samples were then measured and recorded as m_1. The dried samples were soaked in 25°C water for 24 h, after which they were taken out and the water on their surfaces was wiped off with filter paper. Finally, the samples were weighed and the masses were recorded as m_2. The formula for calculating the water absorption is as follows: $f = (m_2 - m_1)/m_1$.

The dielectric analysis experiments were performed using an Agilent 4294A impedance analyzer. The frequency range used for the experiments was 100 Hz–40 MHz. The specimen size was 10 mm × 10 mm.

Preparation of hybrid composites

First, dicyandiamide (2.5 wt % of the total resin), the hardener, and 2-methyl-imidazole (0.15 wt % of the total resin), the accelerator, were dissolved in DMF. The solution was then charged into preweighed brominated epoxy resin, after which OAPS powder was dissolved in THF. The OAPS solution was added to the epoxy resin system with vigorous stirring to produce a homogenous solution. The solid content of the system was about 55 wt %. The mixtures were poured into stainless steel molds with a PTFE film coating. To remove the solvent, all the samples were maintained in a vacuum at 100°C over night. The OAPS content in the nanocomposites were set to 1, 2, 3, 4, and 5 wt %. The systems were cured at 140°C for 1 h and 170°C for 2 h, and post cured at 170°C for 2 h.

RESULTS AND DISCUSSION

Gel analysis

The graph of gel time as a function of OAPS content is shown in Figure 1. All the OAPS-containing nanocomposites displayed prolonged gel times compared with the epoxy resin control. The increase in gel time allows for better control of the curing process conditions of the thermosetting resins and is important to actual production processes. The gel time of the 1 wt % OAPS composites was higher than that of the epoxy resin control. As the OAPS content exceeded 1 wt %, the gel time of the nanocomposites first increased slowly and then gradually decreased. With the addition of OAPS to the epoxy system, POSS cages on the segmental level restrict the motion of the macromolecular chains, enhanced the activation energy of the cocuring reaction, and reduced the reactivity of the system, thus prolonging the gel time. Meanwhile, the amount of amino groups increased with the inclusion of OAPS. Because amino groups have strong reactivity, the average functionality of the systems increased and caused the gel time to decrease. The combined influence of two competing factors greatly increased the gel time initially, and then slightly decreased it with increasing OAPS content.

Morphology of POSS-containing composites

The XRD patterns of POSS-containing composites are presented in Figure 2. No sharp diffraction peaks were observed, revealing no crystal unit structure of

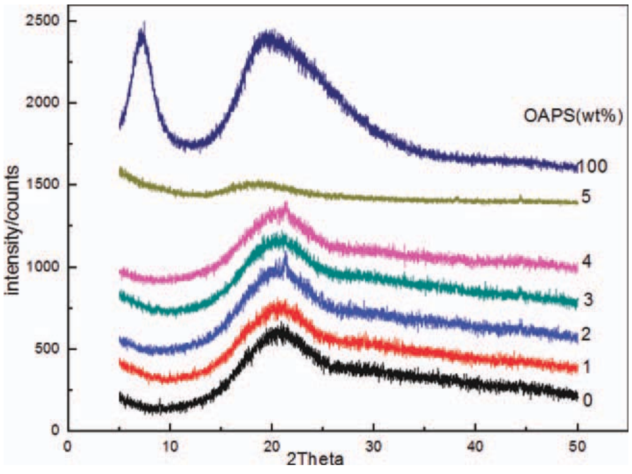

Figure 2 XRD patterns of hybrid composites and pure epoxy resin. [Color figure can be viewed in the online issue, which is available at wileyonlinelibrary.com.]

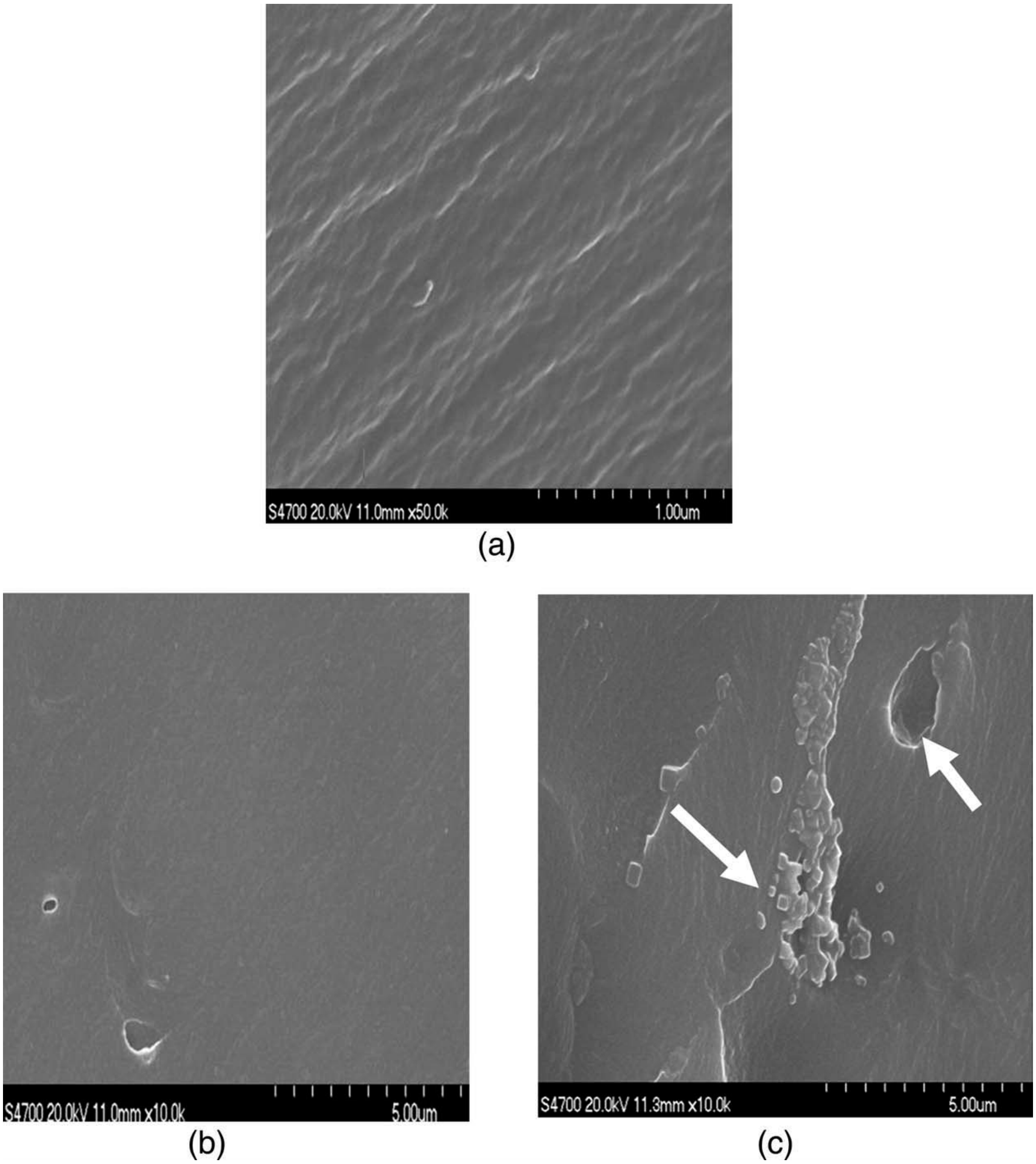

Figure 3 The SEM micrograph of the OAPS/EP nanocomposites with different content: (a) 1 wt % OAPS; (b) 2 wt % OAPS; and (c) 5 wt % OAPS.

OAPS molecules. A strong peak appeared at 7.1° in the OAPS XRD pattern is attributed to the intersilsesquioxane cube distance. The substitution of the amino group on the phenyl ring can occur at the para- or meta-positions, resulting in an OAPS molecule with a variable structure that disrupts crystalline regularity. When the OAPS crosslinked with EP, the attachment of the long-chain epoxy groups to cubic silsesquioxane disrupts the cubic silsesquioxane cage to cage separation structure, resulting the peak at 7.1° disappeared. This is confirmed by the XRD which exhibits the amorphous halos at 19.3°.

Dispersion

The dispersion of OAPS-containing hybrids was investigated using SEM. Figure 3 shows the micrographs of the fracture surfaces of the hybrids. The 1 wt % OAPS composite exhibited featureless morphology with no discernable phase separation

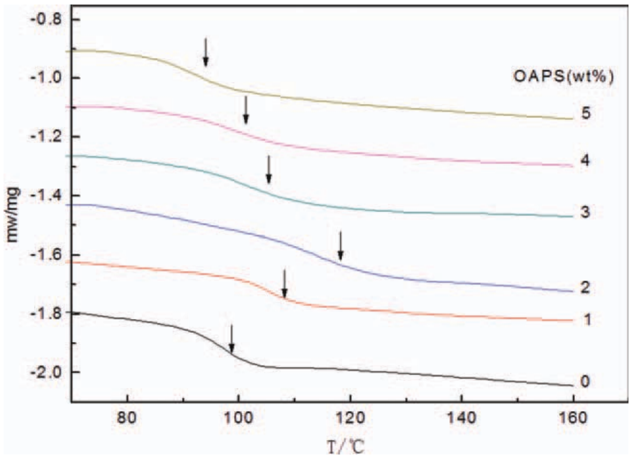

Figure 4 T_g of Epoxy-POSS hybrids varied with different OAPS content. [Color figure can be viewed in the online issue, which is available at wileyonlinelibrary.com.]

[Fig. 3(a)]. In contrast, there is aggregation of OAPS molecules in the continuous epoxy matrix [Fig. 3(b,c)], and the higher the OAPS content, the larger the POSS molecular aggregation phase. In the 5 wt % OAPS composite, some OAPS pores (etched out) and particles (not etched out, the aggregated POSS particles were protected by covered EP to avoid the solvent) were found in the Figure 3(c). This proves that the POSS molecules are involved in the crosslinking reaction and are dispersed uniformly in the epoxy matrix when the POSS molecules have a proper content (in our case not higher than 1 wt %).

Glass transition behavior

All the nanocomposites were subjected to thermal analysis. The DSC curves of control epoxy resin and POSS-containing composites are presented in Figure 4. All the DSC thermograms display single T_gs. The T_g of the OAPS/EP composite increases initially and then decreases with increasing OAPS concentrations. Composites containing 1, 2, 3, and 4 wt % OAPS displayed higher T_gs than the control, whereas the 5 wt % OAPS hybrid had a lower T_g compared with the control epoxy. The increase in T_g could be ascribed to POSS nanoreinforcement of the polymer matrix. In POSS-modified polymers, there are two possible competing factors that determine the T_g of the resulting materials. On the one hand, POSS cages on the segmental level could restrict the motion of macromolecular chains, contributing to the increase in T_g. On the other hand, the presence of bulky POSS cages could increase the free volume of the system and act as internal plasticizers, giving rise to decreases T_g. At low POSS loading levels, the incorporation of POSS may result in polymer chain entanglement because of the good dispersion of POSS, which causes immobility of macromolecular chains and higher T_g. With increasing loading levels, the OAPS particles increase and the effects of the free volume of the hybrids on T_g become greater than those of polymer chain immobility; as such, composites containing 5 wt % POSS showed lower T_g than the epoxy resin control.

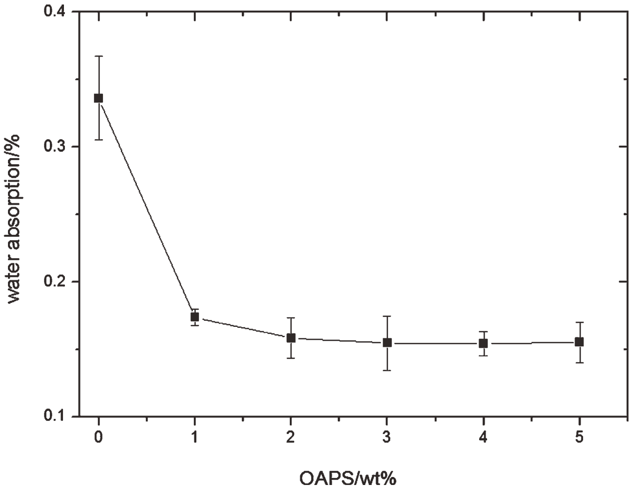

Figure 5 Water absorption with different OAPS content.

Mechanical properties

The data for the impact strength, tensile strength, Young's modulus, and the elongation at break of the hybrids are listed in Table I. Among all the nanocomposites, the 1 wt % OAPS composite had the largest impact strength, tensile strength, and elongation at break, indicating that the inclusion of the proper amounts of OAPS could enhance the fracture toughness and strength of the epoxy matrix. The incorporation of POSS increases the crosslinking

TABLE I
The Mechanical Properties of OAPS/EP Nanocomposites

OAPS (wt %)	Impact strength (kJ/m^2)	Tensile strength (MPa)	Young's modulus (MPa)	Elongation at break (%)
0	47.0 ± 5.1	78.2 ± 9.8	1653.7 ± 134.8	7.0 ± 0.3
1	57.1 ± 5.5	90.3 ± 7.2	2183.3 ± 112.4	7.5 ± 0.4
2	43.8 ± 6.4	86.0 ± 10.3	2395.5 ± 145.3	5.6 ± 0.3
3	17.4 ± 2.0	60.4 ± 8.6	2192.3 ± 155.6	3.5 ± 0.2
4	16.8 ± 2.4	59.2 ± 6.9	2271.4 ± 120.2	3.2 ± 0.2
5	15.8 ± 1.3	48.7 ± 4.4	2287.8 ± 90.7	3.1 ± 0.1

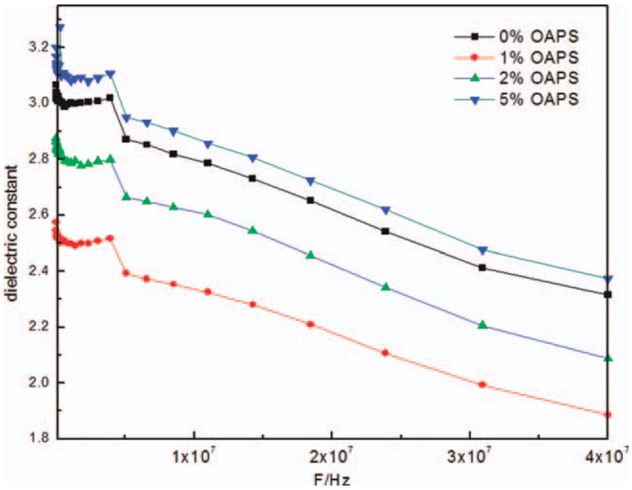

Figure 6 Dielectric constants for epoxy composites containing OAPS. [Color figure can be viewed in the online issue, which is available at wileyonlinelibrary.com.]

density of the resulting nanocomposites and the OAPS has a higher modulus than the EP matrix, which leads to an increase in the impact strength, tensile strength, Young's modulus, and elongation at break of the EP/POSS nanocomposites. The nanocomposites also showed more resistant to moisture. As the OAPS content is further increased, the crosslinking density in the EP/POSS nanocomposites tends to level off. When the OAPS content exceeds 0.1, both the tensile strength and the elongation at break decreases, possibly due to high crosslinking density in the EP/POSS nanocomposites.

Water absorption

The plots of water absorption for the control epoxy and its hybrids containing 1, 2, 3, 4, and 5 wt % OAPS are shown in Figure 5. Compared with the control, the water absorption of the 1 wt % OAPS composite was significantly lower; with increasing OAPS content (>1 wt %), the water absorption of the hybrid composites slightly decreased until it finally approached equilibrium. When 1 wt % OAPS was added to the epoxy resin, the POSS monomers could react completely with the epoxy matrix. Thus, the POSS cages were dispersed in the epoxy matrix at the molecular level and were wrapped by macromolecular chains. This prevents the water molecules from entering the macromolecular chains. Furthermore, the nanostructure of POSS increases the surface area and enhances the interface effect of nanocomposites, causing the hybrids to absorb water mainly by chemical action. However, the POSS molecule is hydrophobic, which reduces water absorption. When the amount of POSS in the reaction system reaches a certain level, the reaction of OAPS molecules with the epoxy resin reaches equilibrium and the content of POSS dispersed in the epoxy matrix at the molecular level remains stable. Thus, water absorption tends to remain in equilibrium with increasing OAPS concentration.

Dielectric constant

The frequency dependence of the dielectric constants of the OAPS/epoxy composites at different loading levels is shown in Figure 6. The dielectric constant of the 1 wt % OAPS composite was reduced by 0.5 compared with the control epoxy resin in the 100 Hz–40 MHz range. With increasing POSS content (>1 wt %), the dielectric constants of the composites increased to a greater degree than that of the control epoxy resin. For polymer composites with fillers, the electrical properties of the fillers and the polymer matrix are usually considerably different, especially in terms of conductivity. These differences can lead to the formation of electrically charged layers at the interfaces; that is, an interfacial polarization when voltage is applied to the materials. Interfacial polarization can cause greater increases in the dielectric constants of polymer composites compared with neat polymers. However, the occurrence of lower dielectric constants in polymer nanocomposites has been reported by several research groups.[29–31] Composites with lower dielectric constants compared with those of neat polymer matrices were observed in some polymer nanocomposites, such as epoxy/TiO_2 and epoxy/ZnO, in which the fillers have higher dielectric constants than the base polymers and interfacial polarization occurs.[29] As such, the possible mechanisms should be examined to explain the lower dielectric constant in the composites. First, the increase in free volume may cause a reduction of the dielectric constant. This increase in free volume may be attributed to the greater steric volume of POSS molecules, which may interfere with efficient chain packing. The correlation between high free volumes and low dielectric constants was previously found in several polymers.[32] The restriction of macromolecular chain movements by POSS particles may be another reason for the reduction of dielectric constants. For polar polymers such as epoxy resins, polymer chain immobility could be one of the important reasons for the reduction of the dielectric constant because the mobility of dipolar groups in epoxy resins contributes to the higher dielectric constant of a composite.[33,34]

At low POSS contents, the incorporation of POSS can effectively restrict the motion of the polymer chain because it can disperse in the epoxy matrix at the molecular level by participating in the crosslinking reaction. This causes the dielectric constants of the hybrid composites to decline. When the POSS content is increased, some POSS molecules not involved in the crosslinking reaction form nanoparticles that separate from the epoxy matrix. This causes interfacial polarization and increases the dielectric constant.

CONCLUSIONS

POSS-containing hybrids of epoxy resin were prepared via a cocuring reaction between octaaminophenyl polyhedral oligomeric silsesquioxane (OAPS) and brominated epoxy resin. The results indicated that the gel time of the 1 wt % OAPS composite was significantly higher than that of the epoxy resin control. XRD and SEM showed that, at the molecular level, the appropriate amount of POSS cages are dispersed in the epoxy matrix because the POSS monomer participated in the crosslinking reaction. DSC and mechanical property test results indicate that the introduction of the proper amounts of POSS could enhance the glass transition temperature, impact strength, tensile strength, and elongation at break of nanocomposites, displaying the nanoreinforcing effect of the POSS cages. The water absorption of the composite significantly decreased initially, and then approached equilibrium as the POSS content increased. The dielectric constant of the 1 wt % OAPS composite was reduced by 0.5 compared with the epoxy resin control in the 100 Hz–40 MHz range.

References

1. Whitesides, G. M.; Mathias, J. P.; Seto, C. T. Science 1991, 254, 1312.
2. Brinker, C.; Scherer, G. Sol–Gel Science: The Physics and Chemistry of Sol–Gel Processing; Academic Press: New York, 1990.
3. Theng, B. K. G. Formation and Properties of Clay–Polymer Complexes, Developments in Soil Science; Elsevier Science: Amsterdam, 1979.
4. Lan, T.; Kaviratna, P. D.; Pinnavaia, T. J. Chem Mater 1995, 7, 2144.
5. Giannelis, E. P. JOM 1992, 44, 28.
6. Giannelis, E. P.; Krishnamoorti, R.; Manias, E. Adv Polym Sci 1999, 138, 107.
7. Schwab, J. J.; Lichtenhan, J. D. Appl Organomet Chem 1998, 12, 707.
8. Feher, F. J.; Wyndham, K. D.; Baldwin, R. K.; Soulivong, D.; Lichtenhan, J. D.; Ziller, J. W. Chem Commun 1999, 999, 1289.
9. Feher, F. J.; Wyndham, K. D.; Soulivong, D.; Nguyen, F. J Chem Soc Dalton Trans 1999, 90, 1491.
10. Lichtenhan, J. D.; Vu, N. Q.; Carter, J. A.; Gilman, J. W.; Feher, F. J. Macromolecules 1993, 26, 2141.
11. Lichtenhan, J. D.; Otonari, Y. A.; Carr, M. J. Macromolecules 1995, 28, 8435.
12. Haddad, T. S.; Lichtenhan, J. D. J Inorg Organomet Polym 1995, 5, 237.
13. Mantz, R. A.; Jones, P. F.; Chaffee, K. P.; Lichtenhan, J. D.; Gilman, J. W.; Ismail, I. M. K.; Burmeister, M. J. Chem Mater 1996, 8, 1250.
14. Haddad, T. S.; Lichtenhan, J. D. Macromolecules 1996, 29, 7302.
15. Gilman, J. W.; Schlitzer, D. S.; Lichtenhan, J. D. J Appl Polym Sci 1996, 60, 591.
16. Romo-Uribe, A.; Mather, P. T.; Haddad, T. S.; Lichtenhan, J. D. J Polym Sci Part B: Polym Phys 1998, 36, 1857.
17. Zhang, C.; Laine, R. M. J Organomet Chem 1996, 521, 199.
18. Lichtenhan, J. D. Comments Inorg Chem 1995, 17, 115.
19. Ni, Y.; Zheng, S. X.; Nie, K. M. Polymer 2004, 45, 5557.
20. Lee, A.; Lichtenhan, J. D. Macromolecules 1998, 31, 4970.
21. Fu, B. X.; Hsiao, B. S.; White, H.; Rafailovich, M.; Mather, P. T.; Jeon, H. G.; Phillips, S.; Lichtenhan, J. D.; Schwab, J. J. Polym Int 2000, 49, 437.
22. Li, G. Z.; Wang, L.; Toghiani, H.; Daulton, T. L.; Koyama, K.; Pittman, C. U. Macromolecules 2001, 34, 8686.
23. Abad, M. J.; Barral, L.; Fasce, D. F.; Williams, R. J. J. Macromolecules 2003, 36, 3128.
24. Choi, J.; Yee, A. F.; Laine, R. M. Macromolecules 2003, 36, 5666.
25. Choi, J.; Kim, S. G.; Laine, R. M. Macromolecules 2004, 37, 99.
26. Fu, B. X.; Namani, M.; Lee, A. Polymer 2003, 44, 7739.
27. Brown, J. F.; Vogt, L. H. I.; Prescott, P. J Am Chem Soc 1964, 86, 1120.
28. Tamaki, R.; Tanaka, Y.; Asuncion, M. Z.; Choi, J.; Laine, R. M. J Am Chem Soc 2001, 123, 12416.
29. Singha, S.; Thomas, M. J. IEEE Trans Dielectr Electr Insul 2008, 15, 12.
30. Roy, M.; Nelson, J. K.; Reed, C. W.; MacCrone, R. K.; Keefe, R. J.; Zenger, W. IEEE Trans Dielectr Electr Insul 2005, 12, 629.
31. Roy, M.; Nelson, J. K.; MacCrone, R. K.; Schadler, L. S. J Mater Sci 2007, 42, 3789.
32. Tanaka, T. IEEE Trans Dielectr Electr Insul 2005, 12, 914.
33. Zhang, J.; Mine, M.; Zhu, D.; Matsuo, M. Carbon 2009, 47, 1311.
34. Lu, J.; Moon, K. S.; Xu, J.; Wong, C. P. J Mater Chem 2006, 16, 1543.